JACC: CARDIOVASCULAR IMAGING VOL. 8, NO. 5, 2015

ISSN 1936-878X/$36.00
PUBLISHED BY ELSEVIER INC. http://dx.doi.org/10.1016/j.jcmg.2014.12.026

RV Longitudinal Deformation Correlates With Myocardial Fibrosis in Patients With End-Stage Heart Failure

Matteo Lisi, MD,*† Matteo Cameli, MD,* Francesca Maria Righini, MD,* Angela Malandrino, MD,* Damiana Tacchini, MD,‡ Marta Focardi, MD, PhD,* Charilaos Tsioulpas, MD,§ Sonia Bernazzali, MD,§ Piero Tanganelli, MD,‡ Massimo Maccherini, MD,§ Sergio Mondillo, MD,* Michael Y. Henein, MD, PhD†

ABSTRACT

OBJECTIVES This study was performed to determine the accuracy of right ventricular (RV) longitudinal strain (LS) in predicting myocardial fibrosis in patients with severe heart failure (HF) undergoing heart transplantation.

BACKGROUND RVLS plays a key role in the evaluation of its systolic performance and clinical outcome in patients with refractory HF.

METHODS We studied 27 patients with severe systolic HF (ejection fraction ≤25% and New York Heart Association functional class III to IV, despite full medical therapy and cardiac resynchronization therapy) using echocardiography before heart transplantation. RV free wall LS, right atrial LS, sphericity index (SI), and tricuspid annular plane systolic excursion (TAPSE) were all measured. Upon removal of the heart, from the myocardial histologic analysis, the ratio of the fibrotic to the total sample area determined the extent of fibrosis (%).

RESULTS RV myocardial fibrosis correlated with RV free wall LS ($r = 0.80$; $p < 0.0001$), SI ($r = 0.42$; $p = 0.01$) and VO_2 max ($r = -0.41$; $p = 0.03$), with a poor correlation with TAPSE ($r = -0.34$; $p = 0.05$) and right atrial LS ($r = -0.37$; $p = 0.03$). Stepwise multivariate analysis showed that RV free wall LS ($\beta = 0.701$, $p < 0.0001$) was independently associated with RV fibrosis (overall model $R^2 = 0.64$, $p < 0.0001$). RV free wall LS was the main determinant of myocardial fibrosis. In the subgroup of patients with severe RV fibrosis, RV free wall LS had the highest diagnostic accuracy for detecting severe myocardial fibrosis (area under the curve = 0.87; 95% confidence interval: 0.80 to 0.94).

CONCLUSIONS In late-stage HF patients, the right ventricle is enlarged, with reduced systolic function due to significant myocardial fibrosis. RV free wall myocardial deformation is the most accurate functional measure that correlates with the extent of RV myocardial fibrosis and functional capacity. (J Am Coll Cardiol Img 2015;8:514–22) © 2015 by the American College of Cardiology Foundation.

Right ventricular (RV) systolic function is an important prognostic factor in heart failure (HF) with longitudinal systolic amplitude of motion and myocardial strain predicting exercise capacity and survival (1–4). Such measurements of RV free wall have proved essential in contributing to 80% of its stroke volume and are able to explain the cavity adaptive mechanisms to volume and pressure overload (5). RV longitudinal and transverse shortening decline also occurs in RV failure in pulmonary arterial hypertension, which in late stages is associated with progressive leftward septal displacement (6,7). The aim of this study was to determine the value of right ventricular longitudinal strain (RVLS) in predicting the extent of RV myocardial fibrosis in patients with end stage HF requiring heart transplantation (HT).

From the *Department of Cardiovascular Disease, University of Siena, Siena, Italy; †Department of Public Health and Clinical Medicine, Umeå University and Heart Centre, Umeå, Sweden; ‡Department of Pathology, University of Siena, Siena, Italy; and the §Department of Cardiac Surgery, University of Siena, Siena, Italy. All authors have reported that they have no relationships relevant to the contents of this paper to disclose.

Manuscript received January 30, 2015; revised manuscript received February 20, 2015, accepted February 20, 2015.

METHODS

STUDY POPULATION. We enrolled 27 patients with end-stage HF (left ventricular [LV] ejection fraction ≤25%; New York Heart Association [NYHA] functional class III to IV despite full medical therapy and cardiac resynchronization therapy [CRT]), referred to Le Scotte Hospital of Siena for a simultaneous right heart catheterization and echocardiographic evaluation before HT (8,9).

Tissue samples of the RV free wall were obtained from explanted hearts. Patients were excluded if they were not in sinus rhythm, on mechanical ventilation, had severe mitral/tricuspid regurgitation, other valve disease, or suboptimal echocardiographic image quality. Patients' echocardiographic results were compared with those from 25 controls, none of whom had a cardiac condition or history of any systemic disease. Patients and controls gave written informed consent before participating in the study. The project complied with the declaration of Helsinki and had been approved by the local ethics committee.

SEE PAGE 523

STANDARD ECHOCARDIOGRAPHY. All echocardiographic examinations were performed according to the recommendations of the American and European Society of Echocardiography (10,11). Studies were performed using Vivid 7, GE Medical System echocardiograph (Horten, Norway), equipped with an adult 1.5- to 4.3-MHz phased array transducer, and an echocardiogram continuously displayed. LV ejection fraction was calculated from the apical views using the biplane modified Simpson method (10) and LV mass using the Penn formula (12) and was indexed to body surface area (BSA).

LV DIASTOLIC FUNCTION. Pulsed-wave Doppler velocities of LV filling were recorded from the apical 4-chamber view by placing the sample volume by the tips of the mitral leaflets. Early (E) and late (A) diastolic LV filling velocities were registered and E/A ratio was calculated (13) and used as standard index of LV diastolic function (14). The LV filling pattern was considered restrictive when the E/A ratio was >2.0, E-wave deceleration time <140 ms, and the left atrium dilated, and >40 mm in diameter (15). Raised E/e' was also taken as a marker of raised filling pressures (16). The same method was used to obtain RV filling velocities and measurements (17).

RV MEASUREMENTS. RV volume was measured from the 4-chamber view at end-diastole. The mid-cavity diameter was measured in the middle third at the level of the LV papillary muscles (18).

RV LONGITUDINAL FUNCTION. RV longitudinal function was studied using the pulsed tissue Doppler imaging technique with the sample volume at the level of tricuspid lateral annulus from the apical 4-chamber view (19). Peak systolic (s'), early diastolic (e'), and late diastolic (a') tricuspid annular velocities were obtained. s' is considered to be a relatively load-independent index of RV longitudinal systolic function, and e' and e'/a' ratio are considered to be load-independent markers of diastolic relaxation. Tricuspid annular plane systolic excursion (TAPSE) was measured with the cursor placed at the lateral angle of the annulus from the apical 4-chamber view (20).

LV AND RV LONGITUDINAL MYOCARDIAL INTRINSIC FUNCTION. LV and RV myocardial function was studied using speckle tracking echocardiography of the apical long axis, obtained from the apical 4- and 2-chamber views, during a quiet breath hold, with a frame rate of 60 to 80 per s. Three consecutive heart cycles were recorded and averaged. The off-line analysis was performed using a commercially available semiautomated 2-D strain software (EchoPac, GE, Waukesha, Wisconsin).

The peak LV longitudinal strain (LS) was defined as the peak negative value on the strain curve. The LV cavity was traced manually from the innermost endocardial edge at end-systole, and the software automatically defined the LS throughout the cardiac cycle. LS was analyzed first in the apical long axis view where the closure of the aortic valve was defined with respect to the R wave to mark end-systole. Then the same process was used for the 4-chamber and 2-chamber views. The automated algorithm provided the longitudinal peak systolic strain value for each LV segment from a 17-segment model polar plot and an average value for the 3 apical views (LV global LS) (21).

Calculation of RV free wall LS was obtained with the same method delineating a region of interest composed of three segments of the lateral wall: basal, mid-cavity, and apical. After segmental tracking, the RV LS curves were generated by the software and the average value of LS was calculated (22) (RV free wall LS [**Figure 1**]).

RV SYSTOLIC FUNCTION. RV sphericity index (SI), was calculated at end-diastole by dividing the short axis by the long-axis diameters (18,23).

RIGHT ATRIAL STRUCTURE AND FUNCTION. Right atrial (RA) area and volume were measured using the biplane method of disks in the apical 4-chamber view at end-systole (10) and were indexed to BSA. RA

ABBREVIATIONS AND ACRONYMS

CRT = cardiac resynchronization therapy

HF = heart failure

NT-proBNP = N-terminal pro-hormone of brain natriuretic peptide

NYHA = New York Heart Association

ROC = receiver operating characteristic

TAPSE = tricuspid annular plane systolic excursion

FIGURE 1 Measurement of Right Ventricular Free Wall Longitudinal Strain

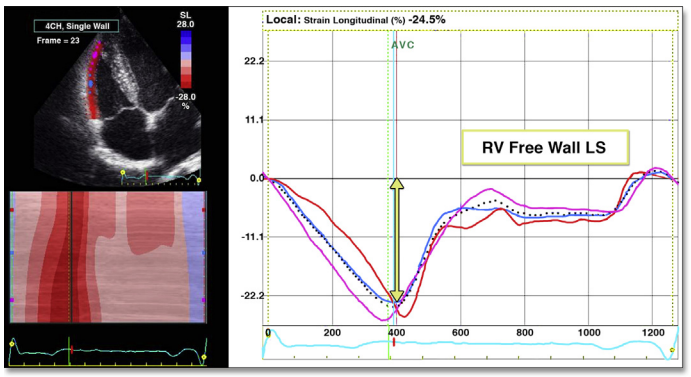

The **dashed curve** represents the average LS of only free wall RV segments along the cardiac cycle. LS = longitudinal strain; RV = right ventricular; AVC = aortic valve closure.

myocardial function was studied from the apical 4-chamber view using the same methods applied for the RV and same frame rate. The RA endocardial border was manually traced, thus delineating a region of interest composed of 6 segments. RA peak atrial longitudinal strain (RALS), measured at the end of the reservoir phase, was calculated by averaging values obtained from all segments (global RALS) (24).

RIGHT HEART CATHETERIZATION. The hemodynamic measurements were performed before the HT. The pressure transducers were balanced before data acquisition with the zero level at mid-axillary line. Pulmonary artery (PA) catheters were used to measure PA pressure (PAP), central venous pressure and RV stroke volume (RVSV), derived by the thermodilution technique (average of 5 cardiac cycles with <10% variation) and by the Fick equation through the sampling of a mixed central venous blood gas obtained from the PA and an arterial blood gas. RV stroke volume index (RVSVI) was calculated by dividing the RVSV by BSA. RV stroke work index (RVSWI) was derived as:

$$\text{RVSWI} = \text{RVSVI} \times (\text{PAPm} - \text{RAPm})$$

where PAPm is mean PAP and RAPm is mean RA pressure. A RVSWI value of 0.25 mm Hg/l · m^2 detected impaired RV function (25).

N-TERMINAL PRO-HORMONE OF BRAIN NATRIURETIC PEPTIDE MEASUREMENT. N-terminal pro-hormone of brain natriuretic peptide (NT-proBNP) was assessed at the time of the right heart catheterization from a peripheral venous blood sample collected in heparin-containing tubes and measured using an electrochemiluminescence immunoassay and the analytic range of the NT-proBNP assay spanned from 5 to 35,000 pg/ml.

CARDIOPULMONARY EXERCISE TEST. Before HT, all patients underwent a maximum cardiopulmonary exercise testing in a lower-limb cycle ergometer (Inbrasport CG-04, Porto Alegre, Brazil), using a graded exercise test with an incremental protocol of 25 watts every minute until exhaustion or symptom development (American Thoracic Society/American

TABLE 1 Patient Clinical Data (n = 27)

Hypertension	20 (74)
Diabetes mellitus	8 (30)
Hypercholesterolemia	19 (70)
Current smoker	2 (7)
NYHA functional class	
III	15 (55)
IV	12 (45)
Cardiomyopathy	
Ischemic	16 (59)
Idiopathic	10 (37)
Hypertrophic cardiomyopathy	1 (4)
Medical therapy	
ACE-inhibitors or ARB	27 (100)
Beta-blockers	25 (93)
Aldosterone antagonists	10 (37)
Loop diuretics	27 (100)
Statins	19 (70)
Amiodarone	11 (41)
Digitalis	6 (22)
CRT-D	11 (41)
Laboratory data	
Hemoglobin (g/dl)	12.6 ± 1.9
Creatinine (mg/dl)	1.28 ± 0.53
Urea (mg/dl)	64.2 ± 39.7
NT-proBNP (pg/ml)	3,846.6 ± 3,213.8

Values are n (%) or mean ± SD.

ACE = angiotensin-converting enzyme; ARB = angiotensin receptor blocker; CRT-D = cardiac resynchronization therapy and defibrillation implantation; NT-proBNP = N-terminal pro-hormone of brain natriuretic peptide; NYHA = New York Heart Association.

TABLE 2 Patient Catheterization Data (n = 27)

Systolic blood pressure, mm Hg	103.0 ± 9.0
Diastolic blood pressure, mm Hg	69.0 ± 9.0
Mean PAP, mm Hg	28.7 ± 7.8
Systolic PAP, mm Hg	39.4 ± 6.8
Diastolic PAP, mm Hg	19.3 ± 3.7
PAoP, mm Hg	22.7 ± 6.3
CI therm, ml/min/m^2	2.1 ± 0.4
CI Fick, ml/min/m^2	1.98 ± 0.3
RVSWI, mm Hg/l · m^2	0.23 ± 0.07

Values are mean ± SD.

CI therm = cardiac index estimated by thermodilution; PAoP = pulmonary artery occlusion pressure; PAP = pulmonary arterial pressure; RVSWI = right ventricular stroke work index.

College of Chest Physicians statement). Oxygen saturation was monitored with pulse oximeter and 12-lead electrocardiogram monitoring was recorded throughout the test. Blood pressure was taken before and at peak exercise. Furthermore, using arterial and venous blood gas analysis we obtained oxygen concentrations at rest and at peak exercise.

During the cardiopulmonary exercise, the exhaled gases were collected by a pneumotachograph attached to a mouthpiece, with concomitant nasal occlusion, and was quantified by a metabolic analyzer (MedGraphics, St. Paul, Minnesota). Gas analysis measurements; oxygen consumption (VO_2), carbon dioxide production, tidal volume, respiratory rate, and minute ventilation were all made. Maximal VO_2 (VO_2 max) was defined by the Fick equation as the product of cardiac output and arterio-venous oxygen difference [$C(a\text{-}v)O_2$] at peak exercise:

$$VO_2\ \text{max} = (HR \times SV) \times [C(a-v)O_2]$$

where HR is heart rate and SV is stroke volume. VO_2 max was measured every minute of exercise, as average of 6 readings and was presented as liter/minute.

HISTOPATHOLOGICAL ANALYSIS. Samples of the RV free wall were obtained after removing the heart. For each patient, 3 full-thickness slices of the RV (basal, mid-cavity, and apical) were obtained and the extent of myocardial fibrosis was calculated as the average of the 3 slices. This analysis was performed to better compare the extent of myocardial fibrosis with RV whole free wall LS strain. Tissue samples were subsequently prepared for histopathological examination. The average sample dimension was 1 × 0.5 cm which was subsequently fixed in 10% buffered formalin, embedded in paraffin, and cut into slices of 4-μm thick for hematoxylin-eosin and Masson's trichrome staining. For Masson's staining, slices were de-waxed with xylol (2 steps, 2 minutes each and soaked into a series of a gradient concentrations from 99% to 95% of alcohol). All slices were washed in distilled water and put in a solution of hematoxylin for 3 min. Subsequently, color change was performed with lithium carbonate (0.1%) to steer the hematoxylin staining. Slices were washed in pure water and colored with Red Ponceau staining (oven at 30°C for 20 s at 45 KW) then put in acid water and phosphomolybdic acid (1 min). The last stage included the addition of green-light and washing with acid water. The ratio of the fibrosis area to the total sample area of each section was used to assess the degree of RV fibrosis (%) as (fibrosis area-total area) × 100 (26).

RV STRAIN MEASUREMENT REPRODUCIBILITY. The software was able to track 146 of 156 (94%) acquired RV segments. Ten patients were randomly selected and Bland-Altman analysis was performed to evaluate the intraobserver and interobserver variability, demonstrating a good agreement with small bias of 0.6 ± 2.9% and 0.8 ± 4.1%, respectively.

TABLE 3 Echocardiographic Data of the Study Population

	Healthy Subjects (n = 25)	Patients (n = 27)	p Value
Female	38	30	ns
Age, yrs	51.8 ± 6.7	53.7 ± 4.6	ns
Heart rate, beats/min	76.9 ± 9.6	79.2 ± 11.2	ns
Body mass index, kg/m^2	25.9 ± 1.9	24.5 ± 2.2	ns
Body surface area, m^2	1.87 ± 0.6	1.99 ± 0.2	ns
End-diastolic LV volume, ml	81.7 ± 11.4	225.4 ± 78.2	<0.0001
LV ejection fraction, %	61.4 ± 1.9	22.3 ± 2.4	<0.0001
LV global LS, %	−21.2 ± 1.9	−8.0 ± 5.1	<0.0001
LV mass index, g/m^2	72.7 ± 12.3	121.8 ± 19.9	<0.0001
Right heart parameters			
Mid-ventricular EDD, mm	24.3 ± 6.2	39.8 ± 4.1	0.002
TAPSE, mm	24.6 ± 3.4	13.3 ± 4.1	0.001
SI	0.36 ± 0.04	0.51 ± 0.07	<0.001
RV length, cm	7.3 ± 0.6	7.9 ± 0.9	ns
Tricuspid E/A ratio	1.67 ± 0.4	1.08 ± 0.9	0.008
Tricuspid s′, cm/s	14.2 ± 2.1	10.6 ± 2.9	0.003
Tricuspid e′, cm/s	13.5 ± 1.9	9.4 ± 0.9	0.001
Tricuspid a′, cm/s	15.6 ± 2.2	11.2 ± 1.2	0.009
Tricuspid e′/a′	0.94 ± 0.1	0.83 ± 0.2	0.03
RV free wall LS, %	−29.7 ± 4.7	−15.3 ± 4.7	<0.0001
RA area, cm^2	14.6 ± 2.4	24.7 ± 3.3	0.006
RALS, %	40.2 ± 12.4	12.2 ± 5.5	<0.0001

Values are % or mean ± SD.

A = atrial trans-tricuspid flow velocity; E = early trans-tricuspid flow velocity; e′ = early diastolic tricuspid annular velocity; EDD = end-diastolic diameters; LS = longitudinal strain; LV = left ventricular; ns = not significant; RA = right atrial; RALS = right atrial longitudinal strain; RV = right ventricular; s′ = tricuspid systolic annular velocity; SI = sphericity index; TAPSE = tricuspid annular plane systolic excursion.

STATISTICAL ANALYSIS. Data are shown as mean ± SD. A p value <0.05 was considered statistically significant. Analyses were performed using the SPSS (Statistical Package for the Social Sciences, Chicago, Illinois) software Release 11.5. Pearson's correlation coefficients were calculated to assess the relationship between continuous variables. The sensitivity and specificity were calculated using standard definition, receiver operating characteristic curves were constructed, and area under the curve was calculated for the prediction of severe RV myocardial fibrosis. Multiple regression analysis was performed to explore the independent determinants of RV fibrosis.

RESULTS

Patient's mean peak VO_2 was 11.2 ± 1.7 ml/kg/min (I° quartile: 9.8 ml/kg/min; II° quartile: 11.2 ml/kg/min

FIGURE 2 Measurement of RV Free Wall LS in a Heart Failure Patient

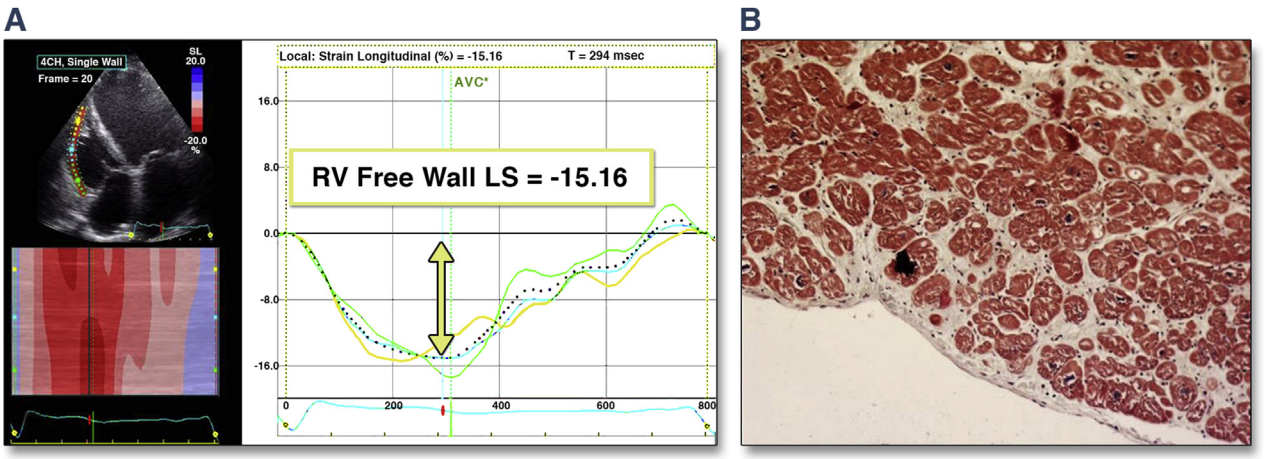

(A) The **dashed curve** represents the average LS of only free wall RV segments along the cardiac cycle. **(B)** RV free wall biopsy in the same patients (original magnification: ×50). Abbreviations as in Figure 1.

FIGURE 3 A Diagram Showing the Increase of Myocardial Fibrosis and the Parallel Reduction of RV Free Wall LS

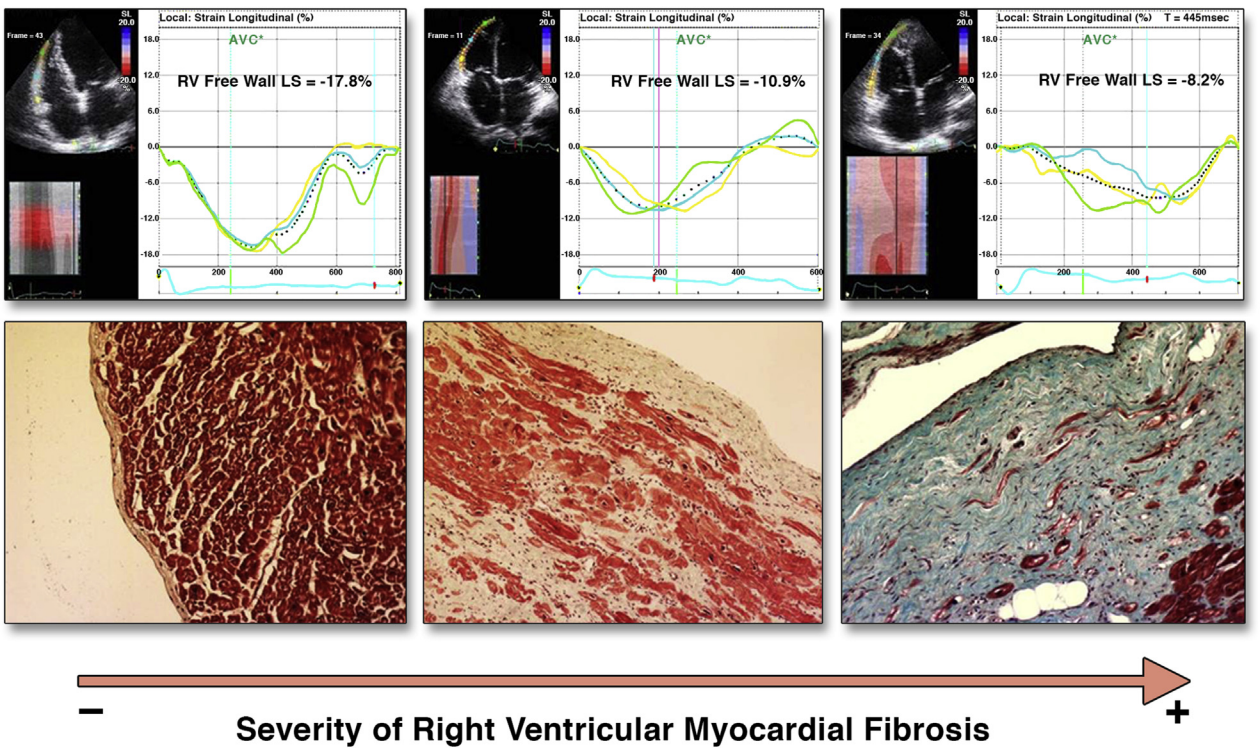

The **dashed curve** represents the average LS of only free wall RV segments along the cardiac cycle. (For RV free wall biopsy, original magnification: ×50.) Abbreviations as in Figure 1.

FIGURE 4 Diagnostic Accuracy of Noninvasive Estimate of Severe RV Myocardial Fibrosis

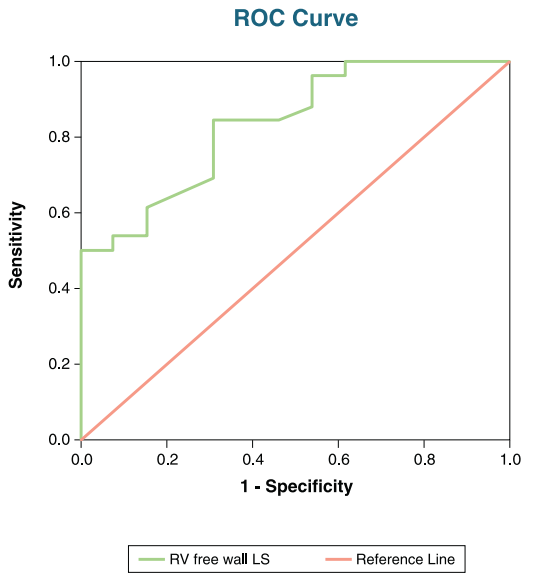

Receiver operating characteristic (ROC) curves for RV free wall LS. Abbreviations as in Figure 1.

[also the median], III° quartile: 12.8 ml/kg/min; IV° quartile: 14.6 ml/kg/min). They had reduced exercise capacity (NYHA functional class III to IV) and elevated NT-proBNP value (I° quartile: 1,545 pg/ml; II° quartile: 3,362 pg/ml [also the median], III° quartile: 5,145 pg/ml; IV° quartile: 10,479 pg/ml) (Table 1). Right heart catheterization data are listed in Table 2. Patients underwent HT 22 ± 14 days after the echocardiographic examination. Seventeen patients (63%) had severe RV myocardial fibrosis (>50%).

FIGURE 5 Correlation Between RV Myocardial Fibrosis and RV Free Wall LS in All Patients

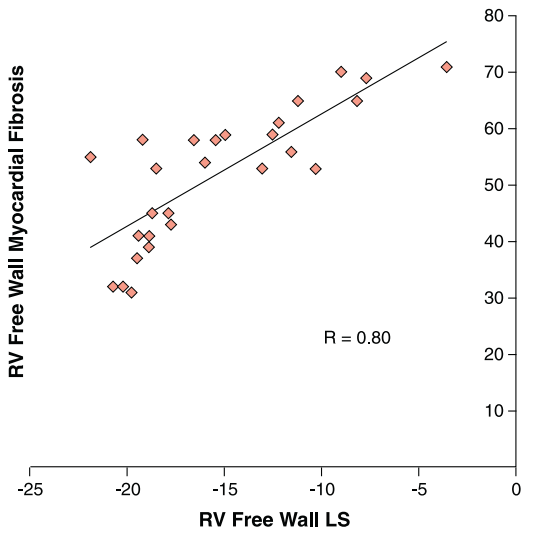

Abbreviations as in Figure 1.

PATIENTS VERSUS CONTROLS. Compared to controls, patients had higher LV mass index ($p < 0.0001$), reduced ejection fraction ($p < 0.0001$) (inclusion criterion) and reduced LV global LS ($p < 0.0001$). LV e′ was lower ($p = 0.002$), whereas E/A and E/e′ were higher ($p < 0.0001$ for both) (Table 3).

Patients had increased RV inlet diameter ($p = 0.002$). RV SI was increased ($p < 0.001$), and E/A and e′/a′ ($p = 0.008$ and $p = 0.03$, respectively) were lower than controls. They also had reduced TAPSE and s′ ($p = 0.001$ and $p = 0.003$, respectively) and RV free wall LS ($p < 0.0001$ for both) and increased RA area ($p = 0.006$) with severely reduced RALS ($p < 0.0001$).

RV FUNCTION VERSUS FIBROSIS. RV myocardial fibrosis correlated with free wall LS ($r = 0.80$; $p < 0.0001$), SI ($r = 0.42$; $p = 0.01$) and VO_2 max ($r = -0.41$; $p = 0.03$), with a poor correlation with TAPSE ($r = -0.34$; $p = 0.05$) and RALS ($r = -0.37$; $p = 0.03$) (Figures 2 to 5, Table 4).

Stepwise multivariate analysis showed that RV free wall LS ($\beta = 0.701$, $p < 0.0001$) was independently associated with RV fibrosis (overall model $R^2 = 0.64$, $p < 0.0001$). RV free wall LS was the main determinant of myocardial fibrosis.

In the subgroup of patients with severe RV fibrosis, myocardial fibrosis correlated with free wall LS ($r = 0.72$; $p < 0.0001$), SI ($r = 0.47$; $p < 0.0001$), RALS ($r = -0.46$; $p = 0.005$), and VO_2 max ($r = -0.44$, $p = 0.01$) with a poor correlation with TAPSE ($r = -0.32$; $p = 0.01$). RV free wall LS had the highest diagnostic accuracy for detecting severe myocardial fibrosis (area under the curve [AUC] = 0.87; 95% confidence interval: 0.80 to 0.94).

LV FUNCTION VERSUS EXERCISE CAPACITY. There was no relationship between LV myocardial deformation (global LS) and exercise capacity (VO_2 max) ($R = -0.29$; $p = ns$).

DISCUSSION

The findings of this study can be summarized as follows: 1) in patients with end-stage HF, the RV is significantly enlarged with reduced systolic function; and 2) RV free wall LS is the best echocardiographic measure that correlates with the extent of myocardial fibrosis.

JACC: CARDIOVASCULAR IMAGING, VOL. 8, NO. 5, 2015
MAY 2015:514–22

TABLE 4 RV Free Wall Myocardial Fibrosis and RV Free Wall LS in All Patients

Patient #	RV Free Wall LS (%)	RV Free Wall Myocardial Fibrosis (%)
1	−16.56	58
2	−10.31	53
3	−12.54	59
4	−15.47	58
5	−11.25	65
6	−11.58	56
7	−19.22	58
8	−16	54
9	−9	70
10	−15	59
11	−12.2	61
12	−8.2	65
13	−7.7	69
14	−3.58	71
15	−17.72	43
16	−17.9	45
17	−21.88	55
18	−18.52	53
19	−13.1	53
20	−18.9	41
21	−20.2	32
22	−18.9	39
23	−19.4	41
24	−19.5	37
25	−18.7	45
26	−19.8	31
27	−20.7	32

Values are (%).
Abbreviations as in Table 3.

DATA INTERPRETATION. RV function in the form of reduced TAPSE has been shown to correlate with exercise capacity and to predict survival in patients with dilated cardiomyopathy and reduced LV systolic function (5,27). In the current study we have confirmed these findings in a group of patients with end-stage HF requiring HT. This gave us a unique opportunity to assess the extent of RV free wall fibrosis histologically, having considered >50% of the myocardial sample as severe fibrosis and compared it with the pattern and extent of RV dysfunction. Among a full battery of RV structure and function measurements, we identified free wall LS as the best predictor of the extent of myocardial fibrosis. Finally, the same parameter predicted the limited exercise tolerance in these patients. Thus, the reduced free wall strain, usually described as impaired intrinsic myocardial function, in fact reflects the severity of segmental fibrosis. Interestingly, there was no similar relationship between LV function and the extent of its myocardial fibrosis.

End-stage myocardial adaptation process is mostly in the form of collagen formation and fibrosis, which when mild, disturbs organ function but when severe it may have significant systemic implications (28). RV response to preload, afterload, or primary myocardial pathology is by cavity enlargement due to its remarkable thin walls compared to the left ventricle (5,6). A behavior that results in significant disturbances to myocardial fiber architecture and interstitial tissue remodeling, localized inflammatory processes, then eventually collagen formation (29) and fibrosis as we have shown. When in a small percentage, the viable segments take over the function, but when severe it results in raised end-diastolic pressure, as was the case in our patients. Because fibrosis is irreversible, it explains the intractable clinical picture of our patients who needed transplantation. Furthermore, in patients with severe myocardial fibrosis, the reduction of functional capacity (VO_2) was closely related to the compromised myocardial performance in the form of RV free wall LS, again supporting the essential role of the RV longitudinal myocardial function in determining symptoms and prognosis of HF (30,31). Unfortunately, our results were unable to ascertain the role of RV free wall LS in establishing the exact levels of function impairment that determine disease progression, from early symptom development to a need for cardiac transplantation, because of the selection bias.

CLINICAL IMPLICATION. This study shows that RVLS is able to estimate RV systolic performance and to predict the extent of myocardial fibrosis in patients with end-stage HF requiring cardiac transplantation. These data can be useful to guide towards optimal medical therapy in HF patients and to identify patients with RV dysfunction before they develop severe irreversible myocardial fibrosis. Having such sensitivity, RV free wall LS could be used to identify patients likely to respond to more aggressive medical treatment, i.e., pressure offloading, compared to those needing an LV assist device implantation (32). Even in the latter, RV free wall LS might stratify patients needing cardiac transplantation rather than a hope for recovery by LV assist device (30).

STUDY LIMITATIONS. The measurements of global and free wall RVLS depend on adequate 2-dimensional apical views to permit an easy delineation of the RV endocardial border and to permit the visualization of the entire RV free wall. Despite these limitations, the RV speckle tracking echocardiography analysis was performed in all patients with good reproducibility. Our study has a limited patient number, despite being a homogenous population.

Eleven patients (41%) had CRT and RV leads, and although this could affect RV systolic and diastolic time relations, it is unlikely to alter intrinsic myocardial function. This claim is supported by previous studies showing that RV apical pacing did not affect RV systolic function, despite induction of electromechanical dyssynchrony (33). Finally, our results cannot propose a cut-off value for RVLS because absolute measurements may be vendor dependent.

CONCLUSIONS

In late-stage HF patients, the right ventricle is enlarged with reduced systolic function due to significant myocardial fibrosis. RV free wall myocardial deformation is the most accurate functional measure that correlates with the extent of RV myocardial fibrosis and functional capacity.

REPRINT REQUESTS AND CORRESPONDENCE: Dr. Matteo Lisi, Department of Cardiovascular Disease, University of Siena, Policlinico Le Scotte, Viale Bracci 1, 53100 Siena, Italy. E-mail: matteo.lisi@hotmail.it.

PERSPECTIVES

COMPETENCY IN MEDICAL KNOWLEDGE: In patients with end-stage HF the RV is enlarged and its systolic function is severely compromised due to significant fibrosis. RV free wall longitudinal strain is the most accurate echocardiographic measure that correlates with the extent of myocardial fibrosis.

TRANSLATIONAL OUTLOOK: If confirmed in large future longitudinal studies, RV free wall longitudinal strain might assist in stratifying patients who need transplantation contrary to those who might benefit from assist devices as a bridge to recovery.

REFERENCES

1. Byström B, Lindqvist P, Henein M. The right ventricle: knowing what is right. Int J Cardiovasc Imaging 2008;24:701–2.

2. Donal E, Coquerel N, Bodi S, et al. Importance of ventricular longitudinal function in chronic heart failure. Eur J Echocardiogr 2011;12:619–27.

3. Cameli M, Lisi M, Righini FM, et al. Right ventricular longitudinal strain correlates well with right ventricular stroke work index in patients with advanced heart failure referred for heart transplantation. J Card Fail 2012;18:208–15.

4. Cameli M, Bernazali S, Lisi M, et al. Right ventricular longitudinal strain and right ventricular stroke work index in patients with severe heart failure: left ventricular assist device suitability for transplant candidates. Transplant Proc 2012;44: 2013–5.

5. Fang F, Henein MY, Yu CM, et al. Right ventricular long-axis response to different chronic loading conditions: its relevance to clinical symptoms. Int J Cardiol 2013;167:378–82.

6. Mauritz GJ, Kind T, Marcus JT, et al. Progressive changes in right ventricular geometric shortening and long-term survival in pulmonary arterial hypertension. Chest 2012;141:935–43.

7. Zhao Y, Henein MY, Mörner S, Gustavsson S, Holmgren A, Lindqvist P. Residual compromised myocardial contractile reserve after valve replacement for aortic stenosis. Eur Heart J Cardiovasc Imaging 2012;13:353–60.

8. Mehra MR, Kobashigawa J, Starling R, et al. Listing criteria for heart transplantation: International Society for Heart and Lung Transplantation guidelines for the care of cardiac transplant candidates—2006. J Heart Lung Transplant 2006; 25:1024–42.

9. Francis GS, Greenberg BH, Hsu DT. ACCF/AHA/ACP/HFSA/ISHLT 2010 clinical competence statement on management of patients with advanced heart failure and cardiac transplant: a report of the ACCF/AHA/ACP Task Force on clinical competence and training. J Am Coll Cardiol 2010; 56:424–53.

10. Lang RM, Bierig M, Devereux RB, et al. Recommendations for chamber quantification: a report from the American Society of Echocardiography's Guidelines and Standards Committee and the Chamber Quantification Writing Group, developed in conjunction with the European Association of Echocardiography, a branch of the European Society of Cardiology. J Am Soc Echocardiogr 2005;18:1440–63.

11. Gottdiener JS, Bednarz J, Devereux R, et al. American Society of Echocardiography recommendations for use of echocardiography in clinical trials. J Am Soc Echocardiogr 2004;17: 1086–119.

12. Devereux RB, Reicheck N. Echocardiographic determination of left ventricular mass: anatomic validation of the method. Circulation 1977;55:613–8.

13. Nagueh SF, Appleton CP, Gillebert TC. Recommendations for the evaluation of left ventricular diastolic function by echocardiography. Eur J Echocardiogr 2009;10:165–93.

14. Quinones MA, Otto CM, Stoddard M, Waggoner A, Zoghbi WA. Recommendations for quantification of Doppler echocardiography: a report from the Doppler quantification task force of the Nomenclature and Standards Committee of the American Society of Echocardiography. J Am Soc Echocardiogr 2002;15:167–84.

15. Nishimura RA, Tajik AJ. Evaluation of diastolic filling of left ventricle in health and disease: Doppler echocardiography is the clinician's Rosetta Stone. J Am Coll Cardiol 1997;30:8–18.

16. Ommen SR, Nishimura RA, Appleton CP, et al. Clinical utility of Doppler echocardiography and tissue Doppler imaging in the estimation of left ventricular filling pressures: a comparative simultaneous Doppler-catheterization study. Circulation 2000;102:1788–94.

17. Sade LE, Gulmez O, Eroglu S, Sezgin A, Muderrisoglu H. Noninvasive estimation of right ventricular filling pressure by ratio of early tricuspid inflow to annular diastolic velocity in patients with and without recent cardiac surgery. J Am Soc Echocardiogr 2007;20:982–8.

18. Rudski LG, Lai WW, Afilao J, et al. Guidelines for the echocardiographic assessment of the right heart in adults: a report from the American Society of Echocardiography endorsed by the European Association of Echocardiography, a registered branch of the European Society of Cardiology, and the Canadian Society of Echocardiography. J Am Soc Echocardiogr 2010;23:685–713.

19. Yu CM, Sanderson JE, Marwick, Oh JK. Tissue Doppler imaging a new prognosticator for cardiovascular disease. J Am Coll Cardiol 2007;49: 1903–14.

20. Lindqvist P, Calcutteea A, Henein M. Echocardiography in the assessment of right heart function. Eur J Echocardiogr 2008;9:225–34.

21. Mondillo S, Galderisi M, Mele D, et al., Echocardiography study group of the Italian Society of Cardiology (Rome, Italy). Speckle tracking echocardiography: a new technique for assessing myocardial function. J Ultrasound Med 2011;30: 71–83.

22. Meris A, Faletra F, Conca C, et al. Timing and magnitude of regional right ventricular function: a speckle tracking-derived strain study of normal subjects and patients with right ventricular dysfunction. J Am Soc Echocardiogr 2010;23: 823–31.

23. Kim HK, Kim YJ, Park JS, et al. Determinants of the severity of functional tricuspid regurgitation. Am J Cardiol 2006;98:236–42.

24. Cameli M, Lisi M, Righini FM, Mondillo S. Novel echocardiographic techniques to assess left atrial size, anatomy and function. Cardiovasc Ultrasound 2012;1:10–4.

25. Matthews JC, Koelling TM, Pagani FD, Aaronson KD. The right ventricular failure risk score. A pre-operative tool for assessing the risk of right ventricular failure in left ventricular assist device candidates. J Am Coll Cardiol 2008;51:2163–72.

26. Cameli M, Lisi M, Righini FM, et al. Usefulness of atrial deformation analysis to predict left atrial fibrosis and endocardial thickness in patients undergoing mitral valve operations for severe mitral regurgitation secondary to mitral valve prolapse. Am J Cardiol 2013;111:595–601.

27. Tan JL, Prati D, Gatzoulis MA, Gibson D, Henein MY, Li W. The right ventricular response to high afterload: comparison between atrial switch procedure, congenitally corrected transposition of the great arteries, and idiopathic pulmonary arterial hypertension. Am Heart J 2007;153:681–8.

28. Plaksej R, Kosmala W, Frantz S, et al. Relation of circulating markers of fibrosis and progression of left and right ventricular dysfunction in hypertensive patients with heart failure. J Hypertens 2009;27:2483–91.

29. Munkhammar P, Carlsson M, Arheden H, Pesonen E. Restrictive right ventricular physiology after tetralogy of Fallot repair is associated with fibrosis of the right ventricular outflow tract visualized on cardiac magnetic resonance imaging. Eur Heart J Cardiovasc Imaging 2013;14:978–85.

30. Cameli M, Righini FM, Lisi M, et al. Comparison of right versus left ventricular strain analysis as a predictor of outcome in patients with systolic heart failure referred for heart transplantation. Am J Cardiol 2013;112:1778–84.

31. Cameli M, Righini FM, Lisi M, Mondillo S. Right ventricular strain as a novel approach to analyze right ventricular performance in patients with heart failure. Heart Fail Rev 2014;19:603–10.

32. Grant AD, Smedira NG, Starling RC, Marwich TH. Independent and incremental role of quantitative right ventricular evaluation for the prediction of right ventricular failure after left ventricular assist device implantation. J Am Coll Cardiol 2012;60:521–8.

33. Nunes MC, Abreu CD, Ribeiro AL, et al. Effect of pacing-induced ventricular dyssynchrony on right ventricular function. Pacing Clin Electrophysiol 2011;34:155–62.

KEY WORDS heart failure, myocardial fibrosis, right ventricle